29th Congress of the International Council of the Aeronautical Sciences
St. Petersburg, Russia; September 7-12, 2014

A THREE-DIMENSIONAL FLAPPING WING MECHANISM FOR WIND TUNNEL EXPERIMENTS

Boyang Li, Bifeng Song, Liguang Wang
School of Aeronautics, Northwestern Polytechnical University, Xi'an, P.R. China, 710072

Keywords: *flapping wing; experiment mechanism; 3-dimentional flap; wind tunnel experiments*

Abstract

For the experimental study about aerodynamic characteristics of flapping wings, especially the unsteady flow at low Reynolds number, a kind of flapping wing mechanism which could achieve complex insect or bird wing kinematics was developed. The design is based on two dual-differential four-bar mechanism and the movement of the wings revolving around 3 axes can be controlled separately. Force and moment measurements were obtained from six-component transducers which are fixed at the root of each wing. A set of control-measure software based on LabVIEW was developed. By accurately control of six brushless motors with this software, different kinds of composite movements can be carried into effect on the wings. The wing with skin and the wing without skin were flapped at the same frequency and kinematics and the two resultant forces were subtracted in order to get the pure aerodynamic forces. The single degree-of-freedom (DOF) and three degrees-of-freedom flapping experiments are conducted in the opening section of a wind tunnel. The aerodynamic forces are compared. The results show that this system is suitable for the future comprehensive wind tunnel experiments to develop high efficient flapping wing and wing kinemics.

1 Introduction

As their potential high aerodynamic efficiency, maneuverability and hover capabilities, Flapping-wing Micro Air Vehicles (FMAVs) shows prospective value in both military and civil fields [1]. Due to the effects of low Reynolds number, the aerodynamic characteristics of flapping wings are quite different from traditional fixed-wings and rotor-wings [2]. The fluid around flapping wings is highly unsteady which cannot be easily described by traditional steady or quasi-steady fluid models [3].

Like the research about other aerodynamic phenomena, the study on aerodynamics of flapping wings can be divided into three ways: theoretic, computational and experimental methods. It is desirable if we get theoretical solutions to any physics process, but the mathematic models of many complicated fluid phenomena, especially the unsteady ones, are so complicated that we have not got general solution at present. Thus, most of study about flapping wings has focused on computational fluid dynamics (CFD) and experimental fluid mechanics in recent years [4].

Studies has shown that the high efficiency of natural flyers is due to their 3-dimensional composite flap [5]. To investigate this, it is common to develop a man-made mechanism equipped with force/torque sensors or flow measure equipment and then analysis the fluid field during different kinds of flap. With geometric and kinematic similarities, one can maintain the dynamic similarity by scaling up the wing dimension while appropriately lowering the flapping frequency, reduced frequency and the Reynolds number [1].

Several researchers have published some similar mechanisms and their experiment results. Ellington et al. [6] developed a robotic model to study the flow over the wing of a hovering hawk moth. They found that leading edge vortex (LEV) plays an important role in the lift-generate of insects. Dickinson et al. [7] built a robotic model to investigate the fluid mechanism of fruit fly. They demonstrated the rotational mechanism and the wake-capture mechanism by directly measurement of forces and visualization of the flow patterns around a flapping wing. Thomson et al. [8] built up an three degrees of freedom experimental apparatus and optimized the flapping wing kinematics. George et al. [9] developed a robotic flapping wing mechanism for use in general studies involving flapping flight and laboratory-based experimental optimization of flapping trajectories. In recent years, Phillips and Knowles [10] conducted an experimental investigation of the spanwise flow development on an impulsively started rotating rectangular wing at 45 deg angle of attack. Vandenheede et al. [2] used force and particle-image-velocimetry (PIV) vorticity measurements of biologically inspired hover kinematics are compared to corresponding results of an unsteady aerodynamic vortex model and a Navier-Stokes (N-S) solver.

In this paper, to investigate the lift-enhancement mechanisms of flapping wings, a kind of 3 degrees-of-freedom flapping mechanism and a set of observe and control software was designed. The flapping mechanism is small enough to be put into small wind tunnel. The software can accurately control the six brushless motors linked to two wings. Some primary wind tunnel experiments were done to verify the functions of this system. The results show that this system can provide researchers with valuable data to examine existed life-enhancement mechanisms in flapping wings and to explore new ones.

2 Flapping Mechanism Design

The mechanism is equipped with two flapping wings. Each wing is designed to have 3 DOFs, as shown in Figure 1 (a). Rotation by ϕ about the X-axis is referred to as the plunge angle; rotation by θ about the Y-axis is referred to as the pitch angle; rotation by ψ about the Z-axis is referred to as the sweep angle. With 3 DOFs of each wing, the mechanism is capable of generating arbitrary flapping patterns to explore lift and thrust force of a single wing and the interaction between two flapping wings such as clap-and-fling theory from Weis-Fogh [11].

The principle of the design is based on dual-differential four-bar mechanism separated by a distance. Two motors are connected to a T-shaped lever by bars and ball joints (Figure 1.b). When the two four-bar mechanisms move in phase, it will lead in-plane plunge motion on the wing. When the two four-bar mechanisms move out of phase, wing pitching is introduced to the flapping wing. The third motor is fixed behind the other two motors. When it drives the entire differential mechanism fore and aft, the wing will sweep around Z-axis (Figure 1.c). Two identical 3 DOF flapping mechanisms are arranged back to back on a plate (Figure 1.d). Then the two wings can flap at the same or different patterns for various experiment purposes.

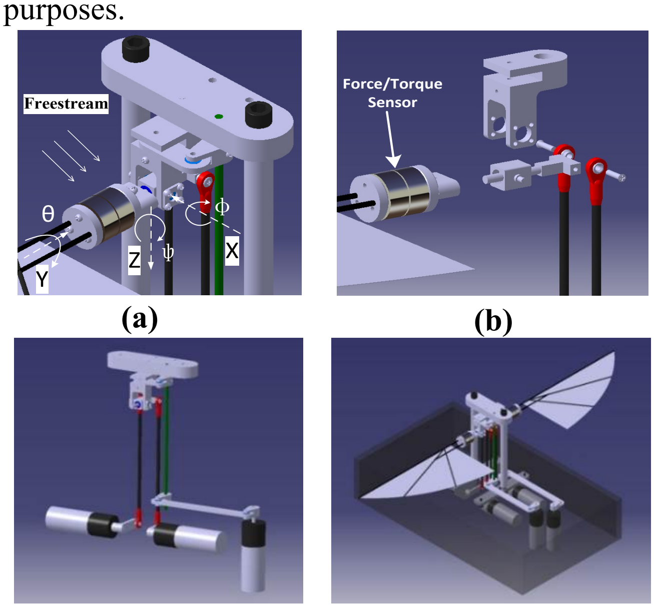

(a) (b)

(c) (d)

Fig. 1 Coordinate definitions and full model of the flapping wing mechanism

The overall material of the mechanism is aluminum and the middle connecting bars are made from carbon fiber. Shaft bearings are installed at each revolution axis. The finished device is compact and stable.

3 Actuation, Control and Measurement

Each DOF is actuated by a brushless DC motor with integrated linear Hall sensor for position feedback. The model of all the 6 motors is Faulhaber_2036 and each of them is driven by a motion controller (Faulhaber MCBL3006C) that receives control instruction from PC via CAN bus. The controller are working at positioning model for moving to defined positions with a high level of resolution. With a PD Controller, the dynamic response can be adjusted to suit the application. The observation and control software was developed in LabVIEW, a graphic programming tool. The motion parameters such as flapping frequency, amplitude of each DOF and lasting time can be inputted at the interface of PC and then the software transforms the motion form into position instructions which will be sent to the motion controllers at high speed.

6-axis force/torque transducers (ATI Nano17 SI-12-0.12) are used to measure the aerodynamic of wings while they are flapping. Analog signals obtained from transducers will be transformed to digital signals by NI USB-6251 DAQ and then digital signals will be transmitted to PC via USB interface. The signals include 3-axis forces and 3-axis torques. The fan controller is connected to PC through RTSI bus in order to control the wind speed of the wind tunnel. All of the experimental system components and signal flows are shown at Figure 2.

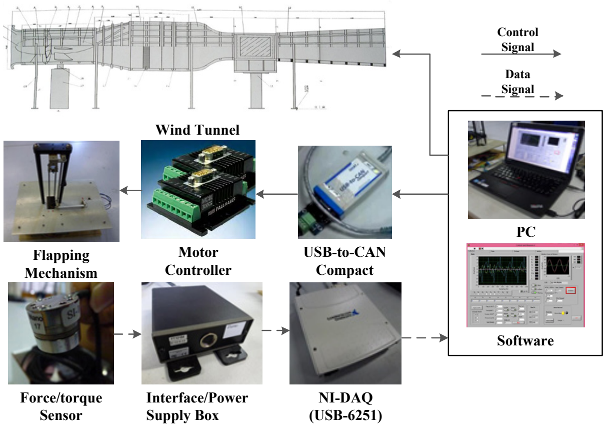

Fig. 2 Instruments of the experimental system

4 Experiment Conditions

To verify the capability of the whole system, primary experiments are performed in the Northwestern Polytechnical University (NPU) MAV Wind Tunnel. The experiments include in-plane flapping force measurement without freestream, in-plane flapping force measurement with a freestream and 3-DOF flapping force measurement with a freestream. Sets of experiment were carried out with different wind speeds, flapping frequencies and motion forms.

4.1 Wind Tunnel

The total length of the tunnel is 6.25m and the wind speed range from 3 to 20 m/s. Experiments are finish at the open section of the wind tunnel since the open section can avoid the influence of wall effects. All of the following experiments and descriptions are based on the single wing form. The overall view of the experimental system is shown in figure 3.

Fig. 3 Overall view of experiment system

4.2 Wing Planform

The flapping wings used in all experiments are two self-designed flexible wings. The wing has a chord of 80 mm and a span of 212 mm. The ribs of the wings are made of carbon fiber poles connected by strings and cyanoacrylate adhesive. The skin covering the wing skeleton is polyether film. Both of the two wings are shown in Figure 4. The wing with membrane can measure both the aerodynamic forces and inertia forces while the wing without membrane can measure only the inertia forces. The pure aerodynamic forces can be obtained by subtracting the results measured by the two wings. The wing is connected with the output bar of the flapping mechanism which is driven by 3 motors. The motors are capable of performing pitch, plunge and sweep motions with a high degree of accuracy.

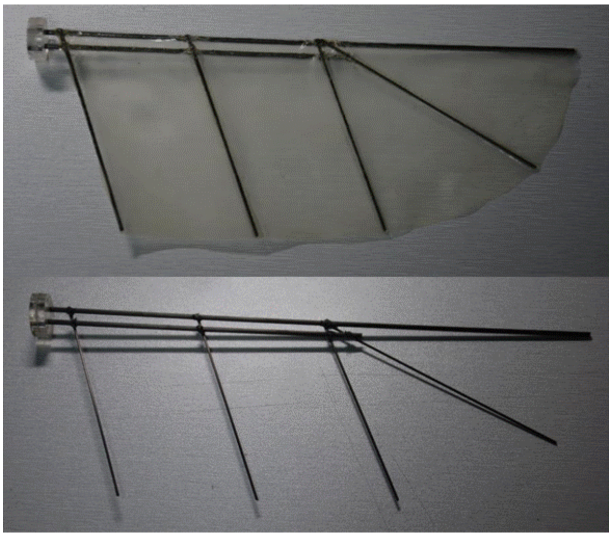

Fig. 4 Wings with membrane and without membrane

4.3 Wing Kinematics

The movements of 3 motors are all sinusoidal curves. The motions of two motors controlling pitch and plunge have the same amplitude A and a differential phase ϕ. The frequency of third motor is 2 times as large as others. Thus, the motion functions of 3 motors are shown as below. The combined movement in the wing is also a sinusoidal move with the plunge amplitude A, pitch amplitude ϕ and sweep amplitude S.

$$P_{M1} = A\sin(2\pi ft) \tag{1}$$

$$P_{M2} = A\sin(2\pi ft + \varphi) \tag{2}$$

$$P_{M3} = S\sin(4\pi ft) \tag{3}$$

4.4 Force Transformation

The main objective of this aerodynamic experimental system is to find flapping trajectories that maximize lift and thrust forces. The lift and thrust are defied in the earth-fixed vertical (z-axis) and forward (y-axis) directions respectively. Then it is necessary to transform the force vectors measured in the wing-fixed frame into the earth-fixed frame. This could be accomplished by Euler angle transformation. The axes are first rotated by angle ψ about the vertical axis, followed by a rotation by angle θ about the horizontal shaft axis, followed by a rotation by angle ϕ about the wing axis. $\mathbf{r}_{wing}$ is referred to as forces or torques measured by transducer directly at the wing-fixed axis. $\mathbf{r}_{earth}$ is referred to as forces or torques that are transformed to earth-fixed axis. The resulting transformation matrix is given by

$$\mathbf{L}_z(\psi) = \begin{bmatrix} \cos(\psi) & \sin(\psi) & 0 \\ \text{-}\sin(\psi) & \cos(\psi) & 0 \\ 0 & 0 & 1 \end{bmatrix} \tag{4}$$

$$\mathbf{L}_y(\theta) = \begin{bmatrix} \cos(\theta) & 0 & \text{-}\sin(\theta) \\ 0 & 1 & 0 \\ \sin(\theta) & 0 & \cos(\theta) \end{bmatrix} \tag{5}$$

$$\mathbf{L}_x(\phi) = \begin{bmatrix} 1 & 0 & 0 \\ 0 & \cos(\phi) & \sin(\phi) \\ 0 & \text{-}\sin(\phi) & \cos(\phi) \end{bmatrix} \tag{6}$$

$$\left[\mathbf{r}_{\text{earth}}\right] = \left[\mathbf{L}_x(\phi)\mathbf{L}_y(\theta)\mathbf{L}_z(\varphi)\right]^{-1} \times \left[\mathbf{r}_{wing}\right] \tag{7}$$

5 Results and Discussions

This chapter shows results of three primary case studies, including comparison between 1-DOF and 3-DOF flapping and comparison between forces results with or without freestream. For the analysis of lift and thrust, forces and torques measured in wind-fixed coordinate are transformed to earth-fixed coordinate. The motion curves of plunge, pitch and sweep angles are shown corresponding with the force curves transported to earth-fixed axes.

5.1 Experiments without Freestream

When flapping frequency is 4 Hz and the plunge angle amplitude is 30 deg, the motion curves around 3 axes and the correspondent lift and thrust are shown in Figure 5. The upside figure shows the motion form of flapping wing defined by three Euler angles. Since this case is the 1-DOF movement, the pitch and sweep angles are close to zero. The downside figure shows force curves that are transformed to earth-fixed axes. Fx and Fz are usually referred to as trust and lift respectively. From the curve, we can notice that the lift is much larger than trust and the forces during upstroke and downstroke are almost symmetrical. By initial analysis, this is mainly due to the high stiffness of the wing rib which has little deformation during flapping. In addition, we can find two clear apexes at each cycle. This phenomenon is possible caused by the added pitch movement which is introduced by the unsymmetrical rotation of the two motors controlling plunge and pitch angle.

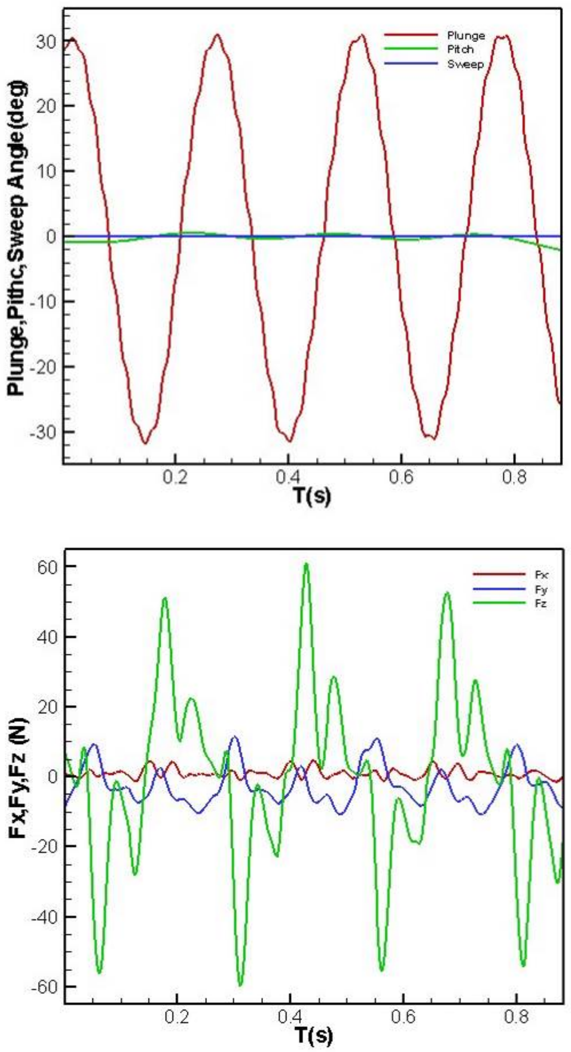

Fig. 5 Motion curve of motors and forces generated by flapping wing

5.2 Experiments with a Freestream

The second case introduced freestream by the wind tunnel. A serious of experiments with different wind speeds are conducted, but here only the results with wind speed of 7 m/s are picked to shown. The motion curve around 3 axes and the correspondent lift and thrust are shown in Figure 6. With the same flapping kinematics but added freestream, we find that the distance between the 'two apexes' is smaller.

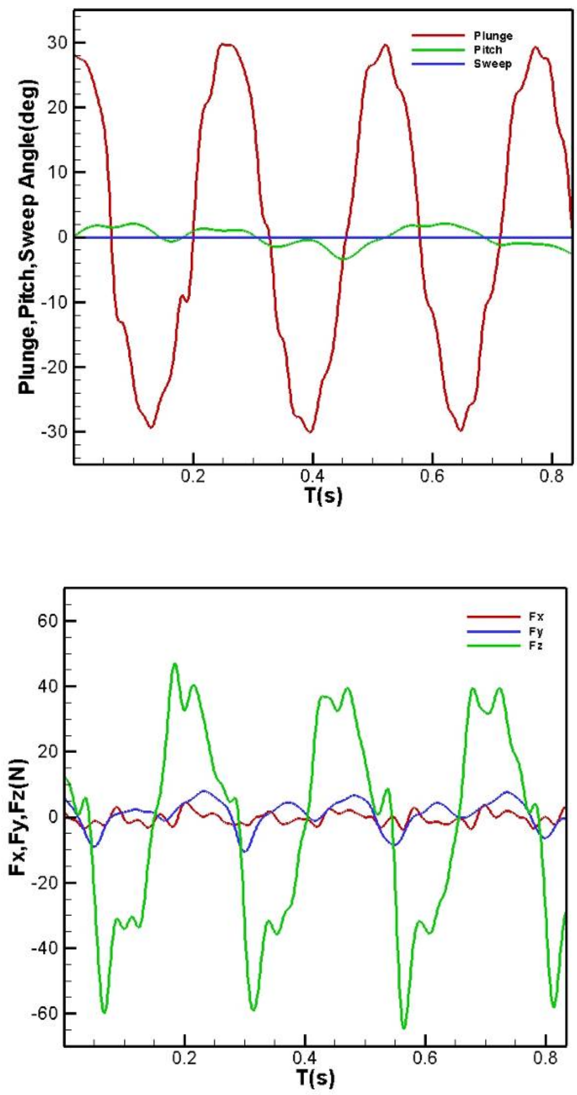

Fig. 6 Motion curve of motors and forces generated by flapping wing

5.3 Experiments with 3 DOF

The last group of figure shows the data of 3-DOF flapping. The flapping frequency is as same as before, which is 4 Hz. The wind speed is 5 m/s. The plunge angle amplitude is 20 deg added with 20 deg of phage lag between two motors and a sweep angle amplitude of 10 deg. The pitch movement is generated by the difference phase of two motors. From the forces curve, we can find that the maximum value of lift is declined while the corresponding value of trust goes up. From the design experience of flapping MAVs, we know that the thrust is the major factor that constrains the overall performance of FMAVs. Thus, it is likely that

3-DOF flap is important to the generation of trust.

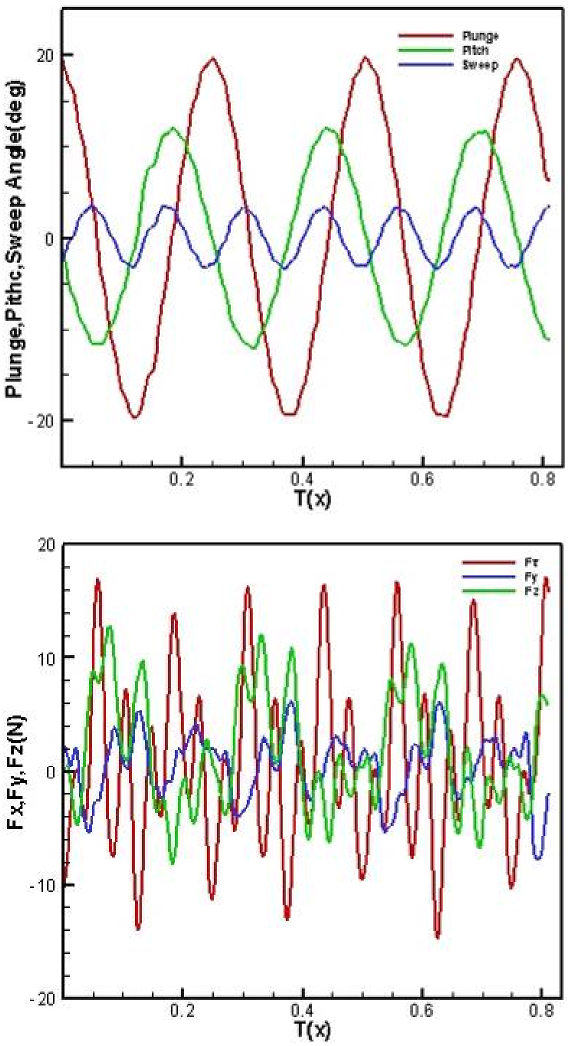

Fig. 7 Motion curve of motors and forces generated by flapping wing

6 Conclusion

In this paper, a kind of 3-DOF flapping mechanism is designed. It can generate complex 3-DOF flapping by precisely control of 3 brushless servo-actuators. Some primary wind tunnel experiments are carried out to verify the reliability and functions of the whole system. From the results of these experiments, we can know that the control-measure system is capable to do further study about the composite motion of flapping wings. More experiments will be done by this system to investigate the three-dimensional aerodynamic of flapping wings in the future.

7 Contact Author Email Address

Contact author: Boyang Li
Email: lbynwpu@gmail.com

References

[1] Shyy W., Lian Y., Tang J., Viieru D., and Liu H. *Aerodynamics of low reynolds number flyers* Cambridge University Press, 2008.

[2] Vandenheede R. B. R., Bernal L. P., Morrison C. L., Gogulapati A., Friedmann P. P., Kang C.-K., *et al.* Experimental and Computational Study on Flapping Wings with Bio-Inspired Hover Kinematics. *AIAA Journal,* pp. 1-12, 2014.

[3] Ho S., Nassef H., Pornsinsirirak N., Tai Y. C., and Ho C. M. Unsteady aerodynamics and flow control for flapping wing flyers. *Progress in Aerospace Sciences,* vol. 39, pp. 635-681, 2003.

[4] Sane S. P. The aerodynamics of insect flight. *J Exp Biol,* vol. 206, pp. 4191-208, 2003.

[5] Platzer M. F., Jones K. D., Young J., and S. Lai J. C. Flapping Wing Aerodynamics: Progress and Challenges. *AIAA Journal,* vol. 46, pp. 2136-2149, 2008.

[6] Ellington C. P. The novel aerodynamics of insect flight: Applications to micro-air vehicles. *Journal of Experimental Biology,* vol. 202, pp. 3439-3448, 1999.

[7] Dickinson M. H., Lehmann F. O., and Sane S. P. Wing rotation and the aerodynamic basis of insect flight. *Science,* vol. 284, pp. 1954-60, 1999.

[8] Thomson S. L., Mattson C. A., Colton M. B., Harston S. P., Carlson D. C., and Cutler M. Experiment-Based Optimization of Flapping Wing Kinematics. presented at the 47th AIAA Aerospace Sciences Meeting Including The New Horizons Forum and Aerospace Exposition, Orlando, Florida, 2009.

[9] George R. B., Colton M. B., Mattson C. A., and Thomson S. L. A Differentially Driven Flapping Wing Mechanism for Force Analysis and Trajectory Optimization. *International Journal of Micro Air Vehicles,* vol. 4, pp. 31-49, 2012.

[10] Phillips N. and Knowles K. Positive and Negative Spanwise Flow Development on an Insect-Like Rotating Wing. *Journal of Aircraft,* vol. 50, pp. 1321-1332, 2013.

[11] Weis-Fogh T. Quick estimates of flight fitness in hovering animals, including novel mechanisms for lift production. *Journal of Experimental Biology,* vol. 59, pp. 169–230, 1973.

Copyright Statement